Theor Chem Acc (2001) 107:48–55
DOI 10.1007/s00214-001-0300-3

Theoretical
Chemistry Accounts

Regular article

Reparameterization of hybrid functionals based on energy differences of states of different multiplicity

Markus Reiher, Oliver Salomon, Bernd Artur Hess

Lehrstuhl für Theoretische Chemie, Universität Erlangen-Nürnberg, Egerlandstrasse 3, 91058 Erlangen, Germany

Received: 13 July 2001 / Accepted: 31 August 2001 / Published online: 16 November 2001

Abstract. Low-spin/high-spin energy splittings for Fe(II) transition-metal complexes – particularly in weak ligand fields – cannot be well described by density functional methods. Different density functionals yield results which differ by up to 1 eV in transition-metal complexes with sulfur-rich first coordination spheres. We attribute this failure to the fact that the high-spin state is systematically favoured in Hartree–Fock-type theories, because Fermi correlation is included in the exact exchange, while Coulomb correlation is not. We thus expect that the admixture of exact exchange to a given density functional will heavily influence the energy splitting between states of different multiplicity. We demonstrate that the energy splitting depends linearly on the coefficient of exact exchange admixture. This remarkable result is found for all the Fe(II)–S complexes studied. From this observation we conclude in connection with experimental results that Becke's 20% admixture should be reduced to about 15% if meaningful energetics are sought for transition-metal compounds. We rationalize that this reduction by 5% will not affect the quality of the hybrid functional since we arrive at a slightly modified functional, which lies between the pure density functional and the hybrid density functional, which both give good results for "standard" systems.

Key words: Adiabatic connection – Hybrid density functionals – Exact exchange admixture – Transition-metal compounds

1 Introduction

Density functional theory (DFT) has been developed to a powerful tool for the calculation of molecules during the last decade. One of its main advantages is that it is – at least to a certain degree – a black box method. Although current density functionals have been developed by adjusting only a few parameters to reference sets of molecules, which do not contain transition-metal compounds, it turned out that these functionals also work quite well for transition-metal compounds, which are hardly tractable by sophisticated ab initio methods. Also, in certain cases DFT can be expected to perform better than coupled-cluster treatments based on single-configuration reference wavefunctions, which are often not realized in transition-metal compounds. Moreover, reliable data for octahedrally coordinated transition-metal compounds with weak ligands can hardly be obtained from accurate ab initio methods with basis sets that are sufficiently large. Single-configuration CCSD(T) calculations using small basis sets, which are occassionally used for comparisons, do not provide proper reference data [1, 2], although this is sometimes assumed as can be seen from the references given in Ref. [3].

Since highly accurate reference data are not available, it is difficult to state which of the results obtained with different functionals is to be preferred. We shall demonstrate this for the splitting between high-spin and low-spin states of several Fe(II)–S complexes. The Fe(II)–S complexes which were selected for this study are shown in Fig. 1.

Considering explicitly the full structure of the ligands in all-electron calculations and following closely the experimental work, we are able to test density functional results by direct comparison with experimental findings. Since for several phosphane ligands PMe_3, PBu_3, PMe_2Ph, and $PMePh_2$ low-spin, diamagnetic ground states have been found [4], we include PMe_3 and PH_3 in our study. The compounds in Fig. 1 were selected since they show a challengingly small singlet–quintet splitting, which is still large enough such that temperature-dependent spin flips cannot be induced.

The article is organized as follows. In the following section we discuss the low-spin/high-spin splittings for the Fe(II) complexes under study in the light of standard density functionals. Subsequently, we analyse the effect of exact exchange admixture on the low-spin/high-spin

Correspondence to: M. Reiher
e-mail: markus.reiher@chemie.uni-erlangen.de

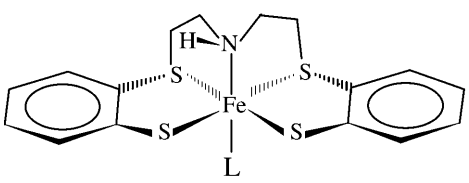

1 (L)
L=NH_3 [50], N_2H_4 [50]

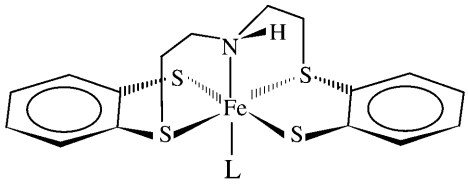

2(L)
L=CO [51], NO^+ [52], PR_3 [4]

Fig. 1. Fe(II)–S complexes $[Fe(N_H)S_4]L$ with ligands L = CO, NO^+, PR_3, NH_3, N_2H_4. The reference to experimental results on these compounds are given in brackets

splitting and arrive at a modified parameter set for the B3LYP functional. The effect on structural parameters is then discussed. The quantum chemical methodology employed is described in detail in the Appendix.

2 $E^e_{LS/HS}$ calculated with standard density functionals

To obtain reliable energetics for reactions with transition-metal compounds, density functional calculations must give the correct multiplicity for the ground state. This is most obvious for those compounds with small energy differences, $E^e_{LS/HS}$, between the low-spin and the high-spin state at their equilibrium structures. Examples of this class of compounds are furnished by Fe(II) complexes in a weak ligand field, for instance, generated by ligands such as thiolates, thioethers and amines.

In the simple picture of ligand field theory we find Fe(II) to be a d^6 case, where all six d electrons may occupy t_{2g} orbitals (in the idealized picture of octahedral symmetry) or are also distributed over the e_g orbitals (Fig. 2). In the former case we would have a singlet ground state and thus a low-spin complex, while in the latter case a quintet ground state and, thus, a high-spin complex results. The energy difference of the states implied by the single–particle picture sketched in Fig. 2 is the low-spin/high-spin energy splitting $E^e_{LS/HS}$. Obviously, triplet states could also be taken into account, but we do not discuss them here since they are not found to be important in the experimental studies.

To illustrate the quantity $E^e_{LS/HS}$, which is probed by quantum chemical methods aiming at the pure electronic contribution, we depict the situation in the simplified sketch in Fig. 3. In this figure, $E^e_{LS/HS}$ is compared to $E^0_{LS/HS}$, which contains the zero-point vibrational energy (ZPVE) difference of the two states and can be measured experimentally. In order to get a rough estimate for the difference of $E^e_{LS/HS}$ and $E^0_{LS/HS}$, we performed a vibrational analysis for **2**(CO) using the BP86/RI method and the valence triple-zeta (TZVP) basis set. We obtained 788.0 kJ/mol for the ZPVE of the singlet state and 794.8 kJ/mol for the quintet state ZPVE. The difference of 6.8 kJ/mol is negligible in this case; however, it should be considered in cases of small $E^e_{LS/HS}$.

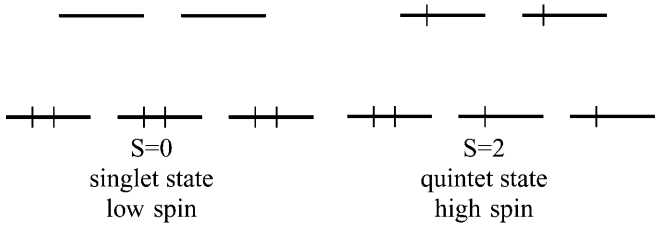

Fig. 2. Single-particle picture of ligand–field theory for the relevance of singlet and quintet states for Fe(II) compounds with d^6 occupation

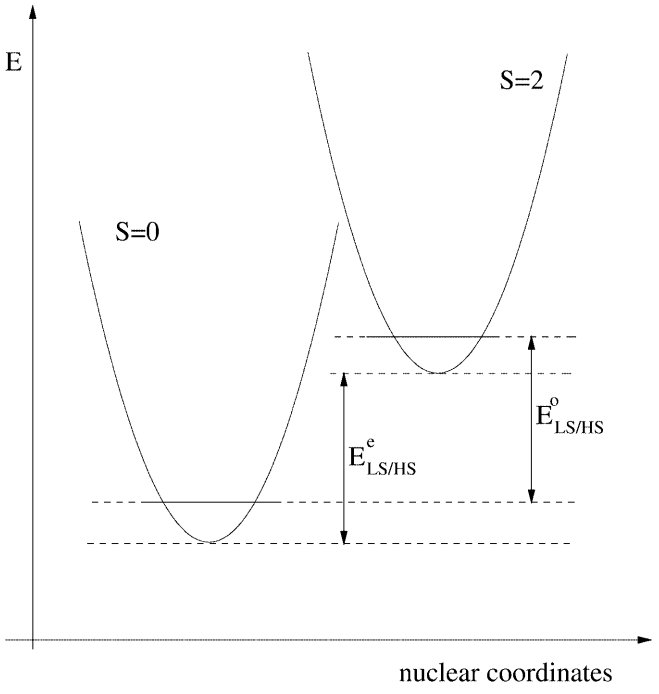

Fig. 3. Scheme for the low-spin/high-spin splitting $E^e_{LS/HS}$, of the electronic states $S = 0$ (singlet, low spin) and $S = 2$ (quintet, high spin). The splitting $E^0_{LS/HS}$ includes at least the zero energy level and can, thus, be compared to experiment. The sign of $E^e_{LS/HS}$ was chosen such that it is positive if the singlet $S = 0$ state is the ground state

The low-spin compound is characterized by singlet multiplicity with total spin quantum number $S = 0$, while the high-spin analogue is described by quintet multiplicity with total spin quantum number $S = 2$. $E^e_{S=0}$ is obtained from restricted Kohn–Sham (KS) calculations, while $E^e_{S=2}$ is extracted from unrestricted KS calculations. In all the cases under study we found only little spin contamination in the unrestricted calculations, i.e., $\langle S^2\rangle \approx S(S+1)$. For example, for the quintet state of **2**(CO) we find a typical value of $\langle S^2\rangle = 6.058$, while the pure spin state would have S(S + 1) = 6.000. This is also reflected in the result that unrestricted KS calculations for the singlet state yield the same result as the

restricted KS calculations. We conclude that the Kohn–Sham model systems are reasonably well represented by a single determinant in both cases. Under these circumstances, the energetics derived from DFT calculations are usually considered to be meaningful.

In very weak ligand fields the spin crossover phenomenon [5–8], i.e., a temperature-dependent spin flip, can be observed. Many of these compounds are known, where Fe(II) is surrounded by a pseudo-octahedral system of six nitrogen atoms as in $[Fe(phen)_2(NCS)_2]$. However, the Fe(II)–S complexes, which are considered in this study, are not of the spin crossover type. This has the important consequence that they do not change their spin state if the temperature is raised from a few Kelvin to room temperature. Therefore, the experimentally determined multiplicity can be taken as the reference multiplicity for the zero-temperature density functional calculation within the unrestricted KS framework.

The energy splittings $E^{e}_{LS/HS}$ for the compounds **1**(L) and **2**(L) obtained with the BP86/RI and B3LYP functionals are given in Table 1. As far as the basis set size is concerned we note that the difference between the split-valence [SV(P)] basis set and the TZVP basis set is relatively small, i.e., about or less than 10 kJ/mol.

Comparing the results from BP86/RI and B3LYP calculations with the experimental findings, we find that none of these functionals are able to predict the correct multiplicity of all ground states. In the case of BP86/RI we find that neither the ammine complex nor the hydrazine complex is obtained as high-spin complexes. On the other hand, B3LYP fails to give the correct ground-state multiplicity for the phosphane complexes. Even in those cases where the correct multiplicity is reproduced by both functionals we cannot extract a reliable value for $E^{e}_{LS/HS}$ since both functionals give splittings that differ by about 120 kJ/mol. In view of these results, we conclude that reliable reaction energetics cannot be obtained for Fe(II) complexes since the errors are of the order of reaction energies.

The question arises whether these results can be generalized for other density functionals. BP86 and B3LYP are typical examples for pure and hybrid functionals and other functionals have not yet been proven to be significantly better [9]. We tested some more functionals, such as PBE [10, 11] and PBE0 [12, 13], from which we conclude that pure density functionals yield results comparable to BP86, while B3LYP furnishes a typical (probably the best) hybrid functional. Furthermore, in studies on ruthenium and manganese complexes we found that the same effect also occurs for these transition metals; however, in these cases the consequences are less serious since Ru(II) compounds are in the low-spin state as a rule, while manganese compounds in the various oxidation states of manganese are often high-spin states, independent of the functional.

We are led to the conclusion that the difference between the BP86 and B3LYP results is typical for pure density functionals versus hybrid functionals and is mostly due to the exact exchange admixture. Consequently, we recall the introduction of exact exchange on the grounds of the adiabatic connection formula and study the dependence of the energy splitting on this admixture.

3 Adiabatic connection and its significance for $E^{e}_{LS/HS}$

The general justification of hybrid density functionals is highlighted by the adiabatic connection formula [14–19],

$$E_{xc} = \int_0^1 E_{xc}^{\lambda}\, d\lambda \ , \tag{1}$$

which describes the connection of a KS system of N noninteracting particles ($\lambda = 0$) with the fully interacting N particle system ($\lambda = 1$) through a continuum of partially interacting systems, where $0 < \lambda < 1$. All these systems have the same density, ρ, being the density of the fully interacting, real system. This formula was utilized by Becke to derive a half-and-half functional [20],

$$E_{xc} = \frac{E_{xc}^{0} + E_{xc}^{1}}{2} \approx \frac{E_{ex.ex.} + E_{xc}^{LSDA}}{2} \ , \tag{2}$$

and later to derive a three-parameter hybrid functional [21]

$$E_{xc} = E_{xc}^{LSDA} + c_1 E_{x}^{B88} + c_2 E_{c}^{PW91} + c_3\left[E_{ex.ex.} - E_{x}^{LSDA}\right] \ , \tag{3}$$

with E_{xc}^{LSDA} being the exchange–correlation functional including the Slater exchange E_{x}^{LSDA}. E_{x}^{B88} is Becke's gradient correction to the local spin density approximation for exchange [19] and $E_{ex.ex.}$ is the exact exchange energy. The parameters $c_1 = 0.72$, $c_2 = 0.81$ and

Table 1. Low-spin/high-spin splittings $E^{e}_{LS/HS}$ (kJ/mol). The singlet state is always taken as the zero-energy reference level. $\Delta E^{e}_{LS/HS} = E^{e}_{LS/HS}$ (BP86/RI) $- E^{e}_{LS/HS}$(B3LYP)

6th Ligand	BP86/RI		B3LYP		$\Delta E^{e}_{LS/HS}$		Exp.
L	SV(P)	TZVP	SV(P)	TZVP	SV(P)	TZVP	
cis-N_HS_4 chelate ligand: 1(L)							
NH_3	37.3	50.3	−62.5	−50.5	99.8	101	high spin
N_2H_4	35.2	50.1	−63.1	−50.8	98.3	101	high spin
trans-N_HS_4 chelate ligand: 2(L)							
CO	150	158	28.0	33.7	122	124	low spin
NO^+	132	134	25.9	39.6	106	94.4	low spin
PMe_3	96.5	105	−24.9	−17.3	121	122	low spin
PH_3	95.1	102	−25.2	−18.1	120	120	–

$c_3 = 0.20$ were fitted to 42 ionization potentials, eight proton affinities and ten total atomic energies of a reference set of molecules containing only first- (i.e., hydrogen), second- and third-row atoms, excluding all transition-metal and heavy-element compounds. Becke used the PW91 gradient correction E_c^{PW91} [22–24] to the correlation functional, although it is now common to use VWN [25] and LYP [26] correlation functionals, E_c^{VWN} and E_c^{LYP}, respectively, defining the B3LYP hybrid functional [27],

$$E_{xc}^{B3LYP} = E_x^{LSDA} + c_1 E_x^{B88} + c_2 E_c^{LYP} + (1 - c_2) E_c^{VWN} + c_3 \left[E_{ex.ex.} - E_x^{LSDA} \right] \quad . \tag{4}$$

There have been many reports devoted to the question of how much exact exchange admixture is needed for a density functional method or how the adiabatic connection should be constructed, respectively, such that chemically accurate structures and energetics are obtained [12, 13, 20, 28–36]; however, these attempts use reference data sets, which do not include a balanced set of transition-metal molecules. In only a few studies were functionals developed by also testing very few transition-metal molecules [37, 38], which are usually very small.

It is well known from ab initio calculations that exchange contributions stabilize those states with higher multiplicities owing to the explicit consideration of Fermi correlation; therefore, it is no surprise that B3LYP always stabilizes the high-spin states, while BP86 favours the low-spin singlet states. Independent of the functional, we found that the hybrid functional low-spin/high-spin splitting differs from the pure density functional result by an approximately constant amount (Table 1).

On the basis of this observation we investigated the splitting as a function of the exact exchange admixture parameter c_3. The result is depicted in Fig. 4 for the Fe(II)–S complexes under study.

First, we note that the results for B3LYP with $c_3 = 0.00$ are very similar to those obtained for BP86/RI (Table 1). This corroborates the conjecture that the difference is mainly governed by the exact exchange admixture.

Figure 4 exhibits the remarkable result that the dependence on c_3 is linear in the range considered. The linearity is perfect for all uncharged complexes, while it is a good approximation for the charged NO^+ species. Moreover, all the straight lines in Fig. 4 are shifted parallel with respect to each other, i.e., the slope of the lines is almost the same, while only the intersections are different. This explains the almost constant difference of $\Delta E_{LS/HS}^e$ between BP86/RI and B3LYP found for different complexes (Table 1).

To analyse Fig. 4 in detail, we start with the strong ligands CO and NO^+, where we find that both BP86/RI and B3LYP (i.e., $c_3 = 0.20$) predict the singlet state to be the ground state. However, the difference in $E_{LS/HS}^e$ amounts to about 120 kJ/mol, which would question any DFT analysis of reaction mechanisms where high-spin transition states could play a significant role. From Fig. 4 we see that B3LYP will give wrong results if $c_3 > 0.24$. In the case of the weak ligands NH_3 and

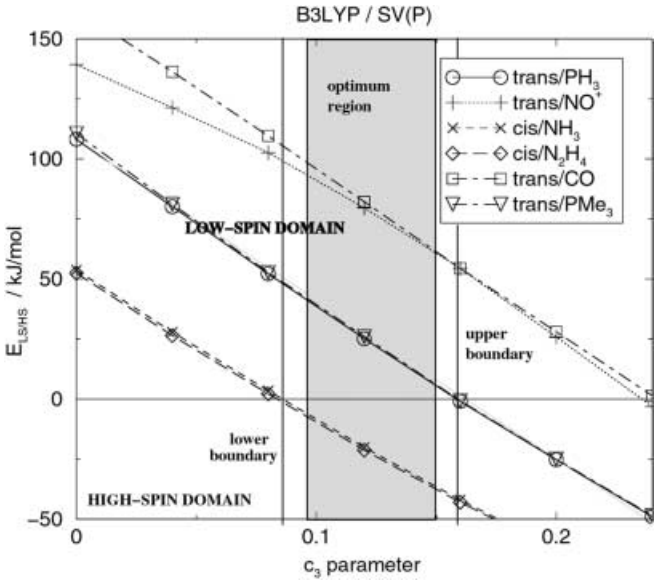

Fig. 4. The low-spin/high-spin energy splittings, $E_{LS/HS}^e$, plotted against the c_3 parameter of the B3LYP functional controlling the exact exchange admixture. The "optimum region" indicates the interval of c_3 values which would yield reliable energetics for Fe(II)–S transition-metal complexes. We chose the value at the upper boundary of this optimum region, i.e., $c_3 = 0.15$, for calculations denoted by B3LYP* (for discussion of this choice see text). The BP86/RI/SV(P) results are found to be very close to the B3LYP($c_3 = 0.00$) values (i.e., on the *y*-axis) as can be seen from Table 1

N_2H_4, for which experiments find high-spin ground states, we find that BP86/RI as well as B3LYP with $c_3 < 0.08$ give the wrong, i.e., a low-spin ground state. This clearly demonstrates that the hybrid functionals are to be preferred and that B3LYP is able to describe the compounds under study provided that c_3 lies in the interval $[0.08, 0.24]$.

It is now instructive to see what happens if stronger ligands such as phosphanes are studied. Here, experiment tells us that the ground state is low spin, but B3LYP in its original parameterization predicts a high-spin ground state. From Fig. 4 it is clear that $c_3 < 0.16$ (a linear regression yields $E_{LS/HS}^e = 0$ for the PMe_3 complex if $c_3 = 0.162$ and a regression coefficient of 0.9992) if the correct ground state is to be reproduced. We are thus led to the conclusion that the exact exchange admixture must be in the interval $[0.08, 0.16]$ in order to yield reliable results. We fix the parameter close to the upper bound in order to keep changes to the original functional as small as possible. $E_{LS/HS}^e = 0$ for PR_3 should be larger than RT in order to make a thermal spin flip unfeasible. For the phosphane complexes, which represent the boundary cases, our choice is an $E_{LS/HS}^e$ in the interval [5 kJ/mol, 15 kJ/mol], which is sufficiently reliable in view of the errors of the density functional methods in general. Note also that the difference of the $E_{LS/HS}^e$ values at the boundaries of the optimum c_3 interval $[0.08, 0.16]$ is less than 30 kJ/mol (if thermal spin flips are excluded for the complexes under study).

For these reasons we chose a value of $c_3 = 0.15$, close to the upper boundary, and denote our B3LYP results obtained with $c_3 = 0.15$ as B3LYP* in the following. The results obtained with this reparameterization are given in Table 2.

By construction, B3LYP* reproduces the experimental findings for all the complexes under study. Note that a reduction of the exact exchange mixing to 15% was also found for a reparameterization of the B97 functional, which considerably improved the energetic predictions of the original B97 functional [39]. Moreover, an exact exchange admixture of $c_3 = 0.16$ was tested for the Bx88/PWc91 functional [30] on the G2 test set, but it was discarded because only little improvement was achieved for the G2 set when compared with other functionals.

We should like to draw attention to the fact that the amount of exchange mixing affects different quantities in different ways. Salzner et al. [40], for instance, adjusted the B3LYP exchange mixing in order to improve the calculated band gaps of polymers and came to the conclusion that c_3 should be increased to 0.30. The reason for this finding is that a particular fault of E_x^{LSDA} is very prominent when calculating differences of orbital energies, which were used to provide a measure for the band gap, namely the lack of self-interaction correction (SIC). Since exact exchange tends to reduce self interaction, the band gaps are corrected in the direction of larger band gaps, which was the desired effect in the case of the work of Salzner et al. SIC is not an important issue when it comes to the differences of total energies. We suggest that for quantities related to orbital energy differences a different remedy for the lack of SIC should be sought.

4 Effect on structural parameters

Since we have dealt with energy quantities only, it now remains to discuss the structural parameters. For this purpose we selected bond lengths since they are more significant and specific than bond angles, which can vary largely upon small structural changes. The B3LYP* optimized structures of the ground states of the six transition-metal complexes are depicted in Fig. 5.

Table 2. Low-spin/high-spin splittings $E^{e}_{LS/HS}$ (kJ/mol). The singlet state is always taken as the zero-energy reference level. B3LYP* denotes B3LYP with $c_3 = 0.15$ and is discussed in Sect. 3

6th Ligand	B3LYP*		Exp.
L	SV(P)	TZVP	
cis-N_HS_4 chelate ligand: 1(L)			
NH_3	−36.7	−24.5	high spin
N_2H_4	−37.7	−25.2	high spin
trans-N_HS_4 chelate ligand: 2(L)			
CO	61.8	67.8	low spin
NO^+	61.5	61.4	low spin
PMe_3	5.7	13.5	low spin
PH_3	5.3	12.3	–

The relevant distances between the metal centre and the first ligand sphere atoms are given in Tables 3 and 4 for the lowest-lying low-spin and high-spin states obtained with BP86/RI, B3LYP, and B3LYP* using two different basis sets.

As expected from ligand field theory, the bond lengths increase upon occupation of e_g orbitals for all the quintet states when compared with the singlet states. All the experimental structures are best reproduced by BP86/RI calculations. The B3LYP bond lengths are acceptable only in a very small number of cases (e.g., for the Fe–S1 distance in *cis*-N_2H_4). In all other cases, the B3LYP distances differ significantly from experiment by up to 15 pm. The B3LYP* structural parameters are close to the B3LYP parameters but are in better agreement with the experimental bond lengths and distances. Thus, B3LYP* yields not only improved energetics but also slightly improved structural data.

In general, BP86/RI yields smaller distances than the hybrid functionals. It is interesting to note that the basis set dependence is rather small, i.e., the bond lengths obtained with the SV(P) basis differ by less than 2 pm from the TZVP bond lengths in most cases.

5 Conclusion

In this work we suggested the use of a modified admixture coefficient for the B3LYP functional in order to obtain reliable reaction energetics for transition-metal compounds. In doing so, we followed a suggestion by Ahlrichs et al. [9], who stressed that ordinary training sets for density functional fits do not contain transition-metal compounds and, thus, do not represent a balanced sample of chemical compounds.

For the Fe(II) compounds selected for this study, we found that pure and hybrid density functionals, for which BP86 and B3LYP are the standard examples, are not able to reproduce reliably the experimentally found multiplicity of the ground state. Associated with this result is the large deviation in calculated low-spin/high-spin splittings of about 100 kJ/mol for BP86 when compared to B3LYP. This almost constant difference was also found for test calculations on ruthenium and manganese complexes, the results of which were not given here, indicating that the findings are of general importance for transition-metal compounds.

The variation of the fit parameter, which determines the amount of exact exchange admixture in hybrid density functionals, reveals that the low-spin/high-spin energy splitting depends linearly on this parameter. Furthermore, all the straight lines were found to be shifted parallel with respect to each other. By comparison with the experimental findings for the complexes under consideration we could determine the value for the exact exchange parameter, namely $c_3 = 0.15$, to which the B3LYP value of 20% should be reduced. For zero exact exchange admixture we found that the B3LYP data give almost the same results as the pure density functional BP86, which demonstrates that large differences for energetics occur between the two classes of pure and hybrid density functionals, but not within one class.

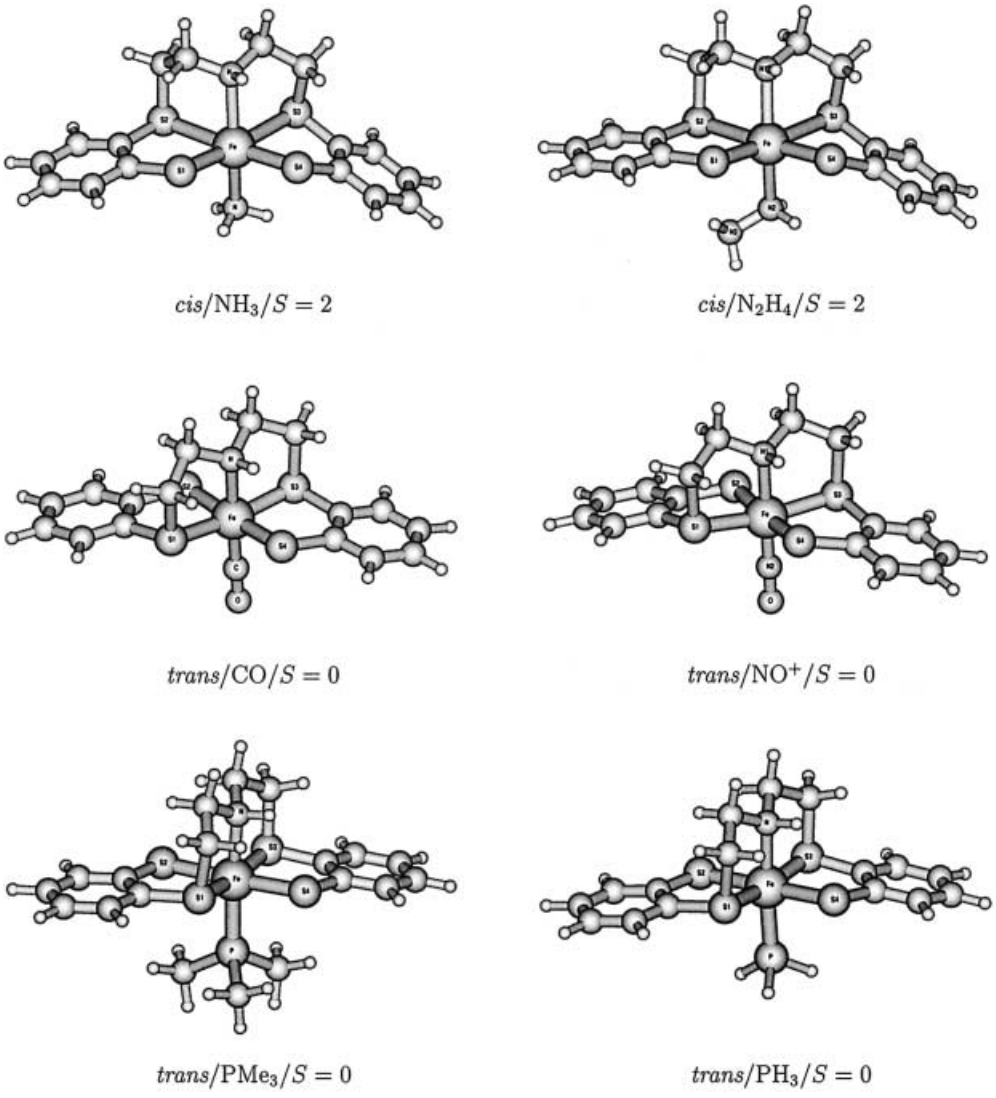

Fig. 5. B3LYP*/TZVP optimized structures of the complexes under study in their ground states (B3LYP* denotes B3LYP with $c_3 = 0.15$)

Table 3. Bond lengths (pm) of ligand atoms in the first ligand sphere of the central iron atom in cis structures **1**(L). S2 and S3 are thioether sulfur atoms, S1 and S4 are thiolate sulfur atoms, N is the amine nitrogen atom in the bridge and *X* denotes the atom of the sixth ligand L that is bound at the iron centre. B3LYP* denotes B3LYP with $c_3 = 0.15$ and is discussed in Sect. 3

	BP86/RI				B3LYP				B3LYP*				Exp.
	SV(P)		TZVP		SV(P)		TZVP		SV(P)		TZVP		
	$S=0$	$S=2$	$S=0$	$S=2$	$S=0$	$S=2$	$S=0$	$S=2$	$S=0$	$S=2$	$S=0$	$S=2$	$S=2$
L = NH_3													[50]
Fe – S1	231.4	233.6	231.6	233.6	236.4	240.1	236.1	239.6	235.2	238.7	235.2	238.3	239.7
Fe – S2	222.4	266.1	224.3	263.8	233.7	272.9	234.3	271.8	230.9	271.6	231.8	270.4	258.8
Fe – S3	222.7	270.0	224.5	269.4	233.9	274.4	234.2	274.0	231.0	273.7	231.9	273.5	258.6
Fe – S4	232.6	236.1	233.3	236.1	237.7	242.2	237.5	241.8	236.3	240.9	236.6	240.4	239.4
Fe – N	205.5	228.6	205.8	230.1	210.5	230.7	210.5	232.0	209.4	230.1	209.6	231.4	224.4
Fe – *X*	202.5	220.4	204.7	223.5	205.7	221.6	207.8	224.1	204.7	221.0	207.0	223.7	218.9
L = N_2H_4													[50]
Fe – S1	230.6	234.5	231.1	233.9	235.5	240.7	235.5	239.7	234.2	239.3	234.4	238.4	240.2
Fe – S2	223.3	263.2	225.0	263.7	234.1	271.3	234.6	270.4	231.6	269.6	232.4	269.4	260.2
Fe – S3	223.4	270.2	225.0	269.5	234.8	275.3	235.2	274.9	232.2	274.3	232.8	274.3	260.2
Fe – S4	234.5	237.2	234.5	237.1	239.2	243.9	239.1	243.0	238.1	242.3	237.9	241.6	238.1
Fe – N	206.8	228.2	206.5	229.5	211.6	230.3	211.7	231.2	210.6	229.7	210.5	230.9	225.5
Fe – *X*	202.3	222.3	203.6	224.9	205.9	223.3	207.5	225.2	205.1	222.9	206.5	225.1	219.2

Table 4. Bond lengths (pm) of ligand atoms in the first ligand sphere of the central iron atom in trans structures **2**(L). S1 and S3 are thioether sulfur atoms, S2 and S4 are thiolate sulfur atoms, N is the amine nitrogen atom in the bridge and *X* denotes the atom of the sixth ligand L that is bound at the iron centre. B3LYP* denotes B3LYP with $c_3 = 0.15$ and is discussed in Sect. 3

	BP86/RI				B3LYP				B3LYP*				Exp.
	SV(P)		TZVP		SV(P)		TZVP		SV(P)		TZVP		
	$S=0$	$S=2$	$S=0$	$S=2$	$S=0$	$S=2$	$S=0$	$S=2$	$S=0$	$S=2$	$S=0$	$S=2$	$S=0$
L = CO													[51]
Fe – S1	224.7	253.9	225.7	253.9	230.9	259.8	231.3	259.6	229.3	258.4	229.8	258.3	222.5
Fe – S2	231.1	241.9	232.2	241.7	234.8	244.9	235.5	244.3	234.1	244.2	234.9	243.9	229.8
Fe – S3	224.7	251.6	225.5	252.2	230.7	258.2	231.0	258.5	229.2	256.7	229.7	257.2	225.1
Fe – S4	232.5	245.9	233.1	244.8	235.8	247.1	236.5	246.1	235.1	247.0	235.6	246.0	230.5
Fe – N	211.3	233.4	210.3	234.2	211.9	231.0	211.3	232.1	211.9	231.6	211.1	233.0	207.2
Fe – *X*	173.4	194.6	174.5	196.6	178.3	209.9	179.6	213.2	176.6	205.1	177.8	208.0	175.3
L = NO^+													
Fe – S1	229.8	255.8	230.2	256.0	232.4	256.3	232.5	240.2	231.9	256.0	232.1	257.1	–
Fe – S2	231.5	235.2	232.2	234.9	233.1	242.2	233.8	224.1	232.9	242.8	233.6	240.5	–
Fe – S3	230.0	251.7	230.3	251.9	232.2	254.6	232.3	239.7	231.9	254.0	232.0	252.9	–
Fe – S4	233.7	236.4	234.5	235.3	234.6	245.1	235.2	224.0	234.4	245.5	235.3	240.8	–
Fe – N	210.9	221.2	210.1	221.1	210.0	229.5	209.5	219.5	210.1	230.0	209.7	228.5	–
Fe – *X*	162.5	179.6	163.9	180.9	162.9	185.1	164.1	319.2[a]	162.7	183.0	163.9	187.7	–
L = PMe_3													[4]
Fe – S1	222.7	254.6	223.6	251.7	230.7	262.7	231.3	262.0	228.5	260.3	229.4	259.8	222.9
Fe – S2	230.3	242.7	231.8	242.7	235.4	246.0	236.5	245.5	234.4	245.9	235.5	245.2	230.7
Fe – S3	222.7	251.4	223.9	255.5	230.6	259.5	231.3	260.2	228.7	258.4	229.5	260.1	223.1
Fe – S4	231.9	249.5	232.9	246.3	237.4	251.7	237.9	250.0	235.8	250.8	236.7	249.0	230.9
Fe – N	210.1	233.1	209.9	234.0	211.9	232.6	211.7	234.5	211.5	232.7	211.3	234.3	206.7
Fe – *X*	221.1	245.1	224.2	249.5	229.9	256.3	232.3	259.4	227.3	253.7	230.1	257.3	221.5
L = PH_3													
Fe – S1	222.7	255.2	224.0	253.5	230.3	261.0	231.0	260.8	228.4	259.6	229.1	258.8	–
Fe – S2	230.3	239.4	231.4	240.5	235.0	243.6	235.8	243.1	233.9	242.6	234.9	242.5	–
Fe – S3	222.8	247.7	224.0	251.1	230.3	258.0	230.9	258.1	228.4	255.9	229.1	256.9	–
Fe – S4	232.1	249.3	233.0	246.3	236.6	248.2	237.3	247.3	235.5	248.8	236.4	246.9	–
Fe – N	207.3	228.9	207.0	229.8	209.2	229.2	208.9	230.9	208.8	229.0	208.5	230.6	–
Fe – *X*	216.6	245.6	219.5	249.2	225.4	263.5	228.3	267.1	222.8	258.9	225.7	263.4	–

[a] The sixth ligand dissociates

Only our new B3LYP* functional with 15% exact exchange admixture is able to reproduce the energetics of all the transition-metal compounds studied here. Additionally, the structural parameters are improved when compared to B3LYP and data from X-ray diffraction. Our analysis is based on the B3LYP functional, but it is easy and straightforward to extend it to other hybrid density functionals, such as B3PW91 or PBE0. Further studies are now in progress to test the general applicability of the B3LYP* functional and to generate a balanced reference data set of transition-metal compounds in order to further evaluate the new parameterization.

Acknowledgements. We are grateful to Prof. D. Sellmann for numerous discussions and helpful comments on experimental findings and peculiarities of the complexes under consideration, which were synthesized in his group.

Appendix

For all the calculations we used the density functional programs provided by the TURBOMOLE 5.1 suite [41]. We employed the Becke–Perdew functional dubbed BP86 [19, 42] and the hybrid functional B3LYP [21, 27] as implemented in TURBOMOLE. Moreover, the resolution of the identity technique was always used for the BP86 functional [43, 44]. All the results were obtained from all-electron restricted and unrestricted KS calculations.

The influence of the size of the basis set was studied by means of two different basis sets. The first was the Ahlrichs SV(P) basis set [45] with polarization functions on heavy atoms, but not on hydrogen atoms. In addition, the TZVP basis set with polarization functions on all atoms was used [46].

For the vibrational analysis, the second derivatives to the total electronic energy were computed as numerical first derivatives [47, 48] to analytic energy gradients obtained from TURBOMOLE. The program MOLDEN [49] was used for the visualization of structures.

References

1. Helgaker T, Gauss J, Jørgensen P, Olsen J (1997) J Chem Phys 106: 6430–6440
2. Bak KL, Gauss J, Jørgensen P, Olsen J, Helgaker T, Stanton JF (2001) J Chem Phys 114: 6548–6556
3. Koch W, Holthausen MC (2000) A chemist's guide to density functional theory. Wiley-VCH, Weinheim

4. Sellmann D, Hofmann T, Knoch F (1994) Inorg Chim Acta 224: 61–71
5. Goodwin HA (1976) Coord Chem Rev 18: 293–325
6. Gütlich P (1981) Struct Bonding 44: 83–195
7. Toftlund H (1989) Coord Chem Rev 94: 67–108
8. König E (1991) Struct Bonding 76: 51–152
9. Ahlrichs R, Furche F, Grimme S (2000) Chem Phys Lett 325: 317–321
10. Perdew JP, Burke K, Ernzerhof M (1996) Phys Rev Lett 77: 3865–3868
11. Perdew JP, Burke K, Ernzerhof M (1997) Phys Rev Lett 78: 1396
12. Adamo C, Barone V (1999) J Chem Phys 110: 6158–6170
13. Ernzerhof M, Scuseria GE (1999) J Chem Phys 110: 5029–5036
14. Harris J, Jones RO (1974) J Phys F 4: 1170
15. Langreth DC, Perdew YP (1975) Solid State Commun 17: 1425–1429
16. Gunnarsson O, Lundqvist BI (1976) Phys Rev B 13: 4274–4298
17. Langreth DC, Perdew JP (1977) Phys Rev B 15: 2884–2901
18. Harris J (1984) Phys Rev A 29: 1648–1659
19. Becke AD (1988) Phys Rev A 38: 3098–3100
20. Becke AD (1993) J Chem Phys 98: 1372–1377
21. Becke AD (1993) J Chem Phys 98: 5648–5652
22. Perdew JP (1991) Phys Res 17: 11–20
23. Perdew JP, Wang Y (1992) Phys Rev B 45: 13244–13249
24. Perdew JP, Chevary JA, Vosko SH, Jackson KA, Pederson MR, Singh DJ, Fiolhais C (1992) Phys Rev B 46: 6671–6687
25. Vosko SH, Wilk L, Nusair M (1980) Can J Phys 58: 1200–1211
26. Lee C, Yang W, Parr RG (1988) Phys Rev B 37: 785–789
27. Stephens PJ, Devlin FJ, Chabalowski CF, Frisch MJ (1994) J Phys Chem 98: 11623–11627
28. Baker J, Muir M, Andzelm J (1995) J Chem Phys 102: 2063–2079
29. Baker J, Andzelm J, Muir M, Taylor PR (1995) Chem Phys Lett 237: 53–60
30. Becke AD (1996) J Chem Phys 104: 1040–1046
31. Ernzerhof M (1996) Chem Phys Lett 263: 499–506
32. Perdew J, Ernzerhof M, Burke K (1996) J Chem Phys 105: 9982–9985
33. Adamo C, Barone V (1997) Chem Phys Lett 274: 242–250
34. Adamo C, Barone V (1998) J Chem Phys 108: 664–675
35. Lynch BJ, Fast PL, Harris M, Truhlar DG (2000) J Phys Chem A 104: 4811–4815
36. Lynch BJ, Truhlar DG (2001) J Phys Chem A 105: 2936–2941
37. Proynov E, Chermette H, Salahub DR (2000) J Chem Phys 113: 10013–10027
38. Hamprecht FA, Cohen AJ, Tozer DJ, Handy NC (1998) J Chem Phys 109: 6264–6271
39. Cohen AJ, Handy NC (2000) Chem Phys Lett 316: 160–166
40. Salzner U, Pickup PG, Poirier RA, Lagowski JB (1998) J Phys Chem A 102: 2572–2578
41. Ahlrichs R, Bär M, Häser M, Horn H, Kölmel C (1989) Chem Phys Lett 162: 165–169
42. Perdew JP (1986) Phys Rev B 33: 8822–8824
43. Eichkorn K, Treutler O, Öhm H, Häser M, Ahlrichs R (1995) Chem Phys Lett 240: 283–290
44. Eichkorn K, Weigend F, Treutler O, Ahlrichs R (1997) Theor Chem Acc 97: 119–124
45. Schäfer A, Horn H, Ahlrichs R (1992) J Chem Phys 97: 2571–2577
46. Schäfer A, Huber C, Ahlrichs R (1994) J Chem Phys 100: 5829–5835
47. Kind C, Reiher M, Neugebauer J, Hess BA (2001) SNF University of Erlangen-Nuremberg
48. Hess BA (2001) NUMFREQ. University of Erlangen-Nuremberg [based on work by Grimme S, Marian C, Gastreich M (1998) University of Bonn]
49. Schaftenaar G, Noordik JH (2000) J Comput-Aided Mol Design 14: 123–134
50. Sellmann D, Soglowek W, Knoch F, Ritter G, Dengler J (1992) Inorg Chem 31: 3711–3717
51. Sellmann D, Kunstmann H, Knoch F, Moll M (1988) Inorg Chem 27: 4183–4190
52. Sellmann D, Kunstmann H, Moll M, Knoch F (1988) Inorg Chim Acta 154: 157–167